Solid Freeform Fabrication 2024: Proceedings of the 35th Annual International Solid Freeform Fabrication Symposium – An Additive Manufacturing Conference
Reviewed Paper

Enhancing Surface Quality in Powder Bed Fusion of 316SS via Shot Peening

Sivasubramanian Chandramouli[a], Michael S. Titus[a], Michael P. Sealy[b*]

[a]*School of Materials Engineering, Purdue University, 701 W Stadium Ave, West Lafayette, IN 47907*
[b]*School of Mechanical Engineering, Purdue University, 585 Purdue Mall, West Lafayette, IN 47907*

* Corresponding author: Tel.: +1 (765) 496-7569. E-mail address: msealy@purdue.edu

Abstract:

Surface topography on additively manufactured components, specifically laser powder bed fusion, is of high concern because it can influence numerous functional properties, such as corrosion resistance, fatigue strength, coating adherence strength, and wear resistance. Further, critical process parameters that drive thermal gradients and solidification rates influence surface topography. Surface treatments are a promising approach to improving surface topography. Therefore, the research objective was understanding material redistribution through cold-working additively manufactured surfaces. The approach was to implement gravity assisted shot peening and pneumatic shot peening on up-skins and down-skins (0-90°) on 316 stainless steels fabricated by laser powder bed fusion. The key outcome was that shot peening improved surface roughness by 50% on average. Also, ideal peening conditions were a function of surface orientation, meaning that the angle and upward/downward orientation required different peening conditions to achieve the same outcome.

Keywords: Additive Manufacturing; Shot Peening; Surface Roughness; Surface Topography

1. Introduction

1.1. Additive Manufacturing (AM)

Additive manufacturing (AM) has profoundly transformed contemporary manufacturing processes, leading to a new era of versatility and efficiency for producing intricate components [1]. It has revolutionized manufacturing strategies for fabricating essential complex components in the aerospace, automotive, and medical industries [2-4]. Additive manufacturing (AM), as defined by ISO/ASTM 52900: 2021 [5], is the production of components using a layer-by-layer material addition technique using powder or wire as the source material. Laser powder bed fusion (LPBF), a subtype of AM, is a process where a laser source selectively fuses regions of the metal powder bed. This method involves the layer-by-layer fabrication of products using a computer-aided design (CAD) model, resulting in exceptional quality and pinpoint accuracy [6]. AM is a near-net shape process, significantly reducing production time and costs by eliminating assembly steps and minimizing waste [7]. With the availability of a wide range of commercially available standard powder bed fusion (PBF) equipment, the final quality and properties of the parts manufactured are influenced by a large number of processing parameters, at least 130 [8]. Key factors affecting the performance of AM components include laser power, scanning speed, hatch spacing, and layer thickness [9]. It was observed that these parameters show a substantial impact on the surface and mechanical properties of the final product [10-11]. Although process parameter

optimization appears viable, it has yet to produce results that meet roughness standards for industry applications [9].

1.2. Role of Orientation on Roughness

The orientation of as-printed components, a critical aspect of AM, plays a pivotal role in determining mechanical properties [12]. Consequently, there is a pressing need to focus on non-destructive post-processing methods to enhance these properties in metallic three-dimensional printed samples. The high initial roughness of 316SS material, ranging from 10 to 15 μm [13], surpasses the standard requirements for direct application in aerospace industries, which typically demand a roughness of about 1 μm [14]. High roughness leads to localized stress concentration points [15], crack generation [16], and low service life [17] of the parts. The current emphasis is on machined surfaces, and remarkably, shot peening on AM samples remains underexplored. Surface enhancement techniques through cold working generate a layer of compressive stress due to surface deformation. This state-of-the-art technology offers a dual advantage on AM samples compared to machined ones, as it reduces roughness and transitions tensile residual stress from the as-built state to compressive stress.

1.3. Shot Peening as a Post-processing Step

This work explores shot peening as a post-processing method to reduce roughness, increase surface compressive residual stress, and improve surface finish. Shot peening is a prominent method in aerospace and automobile industries to enhance surface integrity via cold working. It is a cold working process that helps to increase the strength of parts through surface plastic deformation, closing surface pores or cracks [18]. The main process parameters of shot peening are the bead size and material, Almen intensity, and coverage. The Almen intensity measures the peening intensity obtained by the “Almen” test [19]. The shot size plays a vital role in the final surface finish obtained. This is because it influences the impact energy and the diameter of the impression, which is directly proportional to the diameter of the shot [20]. The selection of the bead material plays a crucial role in the effect of surface enhancement. This work focuses on gravity assisted shot peening (GASP) and pneumatic shot peening (PSP). The main difference between these methods is the energy source and the media size. This significantly affects on roughness, directly influencing the plastic deformation achieved on the as-printed surface with sharp peaks and valleys. Adding to that, optimization of peening parameters in GASP was necessary due to limited application history and lack of research, which was done with the help of progressive surfaces before finalizing and proceeding with the peening.

The selection of bead material for shot peening 316SS is critical. Variations in bead composition from the substrate can lead to iron contamination. Additionally, using beads with higher hardness than the substrate can result in bead breakage and residue accumulation, leading to inhomogeneous surfaces on the treated parts. Therefore, careful consideration of bead material and hardness is essential to maintain surface integrity and avoid contamination [21].

The effect of shot peening on as-built LPBF components on surface roughness, residual stress, and microstructure has not been well studied. A study from Gundgire *et al.* [22] considered varying coverage from 100% to 4200% and investigated the surface roughness in both as-machined and as-printed components using the same shot peening parameters. For as-machined samples, the

initial surface roughness was 0.2 µm, and roughness increased to 5.5 µm after shot peening with 100% coverage. However, increasing the coverage up to 42x reduced the surface roughness to 4.21 µm. Conversely, additively manufactured (AM) samples initially exhibited an as-built surface roughness of 8.8 µm. The surface roughness was reduced to 5.8 µm after standard shot peening. After increasing the coverage to 42x, the surface roughness further decreased to 3.8 µm. This work showed that shot peening could roughen surfaces already smooth (such as machined) or smoothen surfaces already relatively rough (such as as-built LPBF). However, the analysis on oriented surfaces has not been explored.

The differences in surface topography also reflected these changes in surface roughness values. In the as-machined scenario, the shot peening process introduces imprints from the beads, increasing surface roughness. In contrast, when dealing with AM parts, the initial as-printed surface exhibits highly random surface patterns with sharp peaks and deep valleys. However, shot peening mitigates these irregularities, refining surface texture. These insights shed light on the multifaceted influence of shot peening, demonstrating that it can lead to comparable final surface roughness levels for machined and AM surfaces despite their distinct initial roughness characteristics [22]. Żebrowski *et al.* [23] worked on the effect of shot peening on DMLS-based Ti-64 samples where roughness reduction observed was around 33%, and CrNi steel beads have high hardness (79 HRC), which affects the peening effects and adds a damaging effect more than surface enhancement. One positive aspect of shot peening is that internal channels such as holes and hollow parts can also be processed like exterior surfaces due to the small bead size and accessibility of surfaces through proper guiding of media during peening. Although different materials and sizes of beads are analyzed, optimizing the peening condition through exposure time and intensity is poorly understood.

Table 1 presents an overview of the impact of peening on final surface roughness. Although significant reductions in roughness were achieved by multiple researchers, none of the methods met the industry standard requirement of 1.6 µm [14]. This shortfall can be attributed to the broad approach to the peening process and the incomplete utilization of the fundamental principles and parameters governing the technique. Therefore, a comprehensive review and optimization of peening processes is necessary to maximize their efficacy and achieve the desired surface quality standards.

Table 1: Summary of the effect of shot peening on additively manufactured 316SS

Bead media	Bead size (mm)	Coverage	Roughness (µm)		References
			Initial	Final	
Cast steel shots	1.0	200% in 15mins	10.0	5.3	Sugavaneswaran *et al.*, 2018, Surfaces and Interfaces [24]
Cast steel shots	1.0	200% in 15mins	-	2.8	Maleki *et al.*, 2021, Metals and Materials International
Glass beads	0.25	58psi for 120secs	21.2	4.1	Wood, 2019, MDPI [25]
Martensitic chromium media	0.62	107.3psi for 42 passes	8.8	3.8	Gundgire *et al.*, 2022, Materials characterization [22]
250 Zirconium oxide	5.0	Water jet 10MPa for 20mins	17.3	2.9	Behjat *et al.*, Materials Today: Proceedings [26]
1) Al2O3 + 2) Glass	0.12	1) 50 psi for 30s 2) 55 psi for 30s	4.0	1.2	Klotz *et al.*, 2018, Int J. of Fatigue [27]
1) Cast steel shots 2) Glass beads	1) 0.58 2) 0.12	CSP (100%) & SSP (1000%)	4.5	3.7	Bagherifard *et al.*, 2016, Materials and Design [28]

2. Materials and Methods

2.1 Powder and Printing Conditions

Truncheon specimens were fabricated with step-wise inclinations at 10° to facilitate analysis of surface topography and roughness before and after shot peening at varying inclination angles, as shown in *Figure 1(a)*.

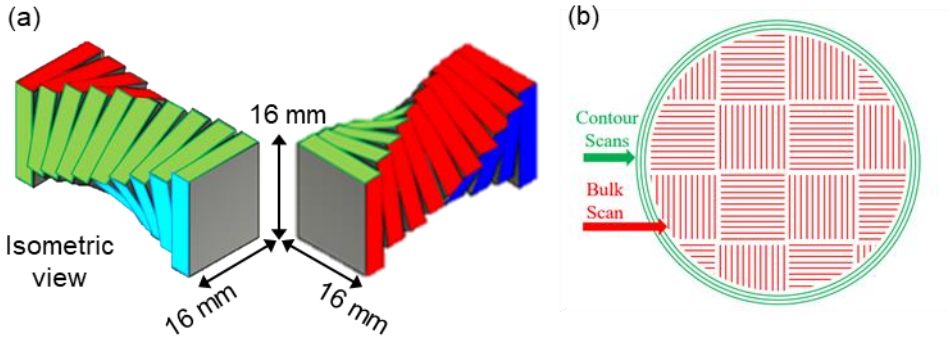

Figure 1: (a) Truncheons and (b) scan strategy.

The 316SS truncheon samples were printed using a Lumex Avance-25 SLM machine (Matsuura, USA) with the optimized printing conditions (shown in

Table 2) with low layer thickness and optimum energy density based on previous history with excellent quality and high accuracy. The rotation angle with each layer of AM was selected to be 67°, which helps to improve adhesion between layers and minimize delamination and anisotropy. This further helps in developing finer grains and minimizes defects [29].

The outer skin of the samples was scanned in a unique method compared to the bulk sample as shown in *Figure 1(b)*. Rescanning helps to remelt the outer surface, filling in gaps or uneven areas created during the initial scan. This results in a smoother and more uniform surface finish [30]. In this research, the contour scan was scanned twice the number of times as that of the bulk samples. Furthermore, five measurements on each surface were considered for analysis to increase reliability. Six truncheons underwent Gravity Assisted Shot Peening at 7A, and six truncheons underwent Pneumatic Shot Peening at a unique intensity with two samples in each subtype of intensities: 1.9A, 4.6A, and 6.9A.

Table 2: Printing parameters for 316SS truncheon samples

Process parameters	Lumex Avance-25	
	Raster	Vector
Laser power (W)	320	
Scanning speed (mm/sec)	1000	2000
Layer thickness (µm)	50	
Hatch spacing (µm)	120	150
Volumetric energy density (J/mm^3)	53.3	21.3
Rotation with each layer (°)	90	
Table temperature (°C)	150	

2.2 Shot Peening

The peening process is performed using cast steel spherical beads. For gravity assisted shot peening, the standard bead size was 1.8 mm, and for pneumatic shot peening, it was 0.178 mm. GASP is performed with an intensity of 7A by Progressive Surfaces, and PSP was done at three distinctive intensities of 1.9A, 4.6A, and 6.9A at Sinto America with spherical steel shots.

Figure 2 illustrates the improvement in surface quality of additive-manufactured parts through different post-processing methods. Initially, the as-printed surface exhibits significant roughness with pronounced peaks and valleys. Post-processing with PSP reduces this roughness by smoothing out many surface irregularities. Further improvement is achieved with GASP, which results in an exceptionally smooth finish. The comparison clearly shows how each subsequent treatment method significantly enhances the surface quality of the parts. Another significant difference between GASP and PSP is the media size, as shown in *Figure 2*. GASP uses a media size ten times larger than PSP, influencing on the peening depth and plastic deformation.

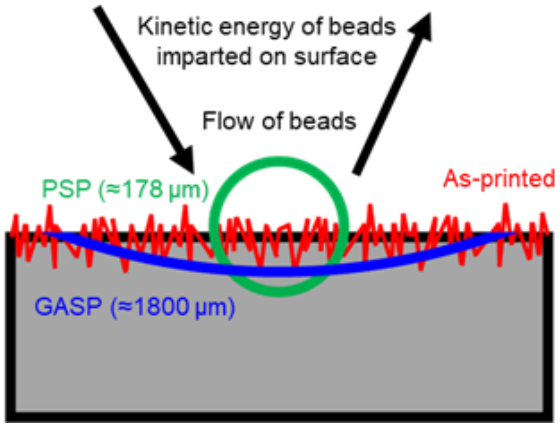

Figure 2: Schematics of gravity assisted shot peening versus pneumatic shot peening.

There are two critical parameters in the case of gravity assisted shot peening: the peening height (H), which is the height at which the beads are dropped, and the peening time (T). Thus, based on the parameters, the peening operation was performed at multiple time intervals at two specific peening heights, 60 and 85 inches. When performing the peening at 60 minutes, the raster still persisted on the surface, which was removed when the peening height was increased to 85 inches. Further, choosing the height at 85 inches, GASP was performed for the time period of 5, 10, 20, 40, and 60 minutes for analysis, and the effect of peening was negligible when the peening was done for 5, 10, 20 minutes which gets to a moderate reduction in roughness when moving to 40 minutes and finally reached saturation when increasing the period from 40 to 60 minutes. For PSP, the process is more standardized and easily implemented with better controllability and uniformity. Due to the difference in roughness, the down-skins have been peened twice the peening time as the up-skins in the case of GASP.

2.3 Surface texture characterization

The measurement of surface areal parameters at complex orientations and different materials was performed using a white light interferometer (Zygo Zescope), which gives a detailed understanding of the surface topography of additively manufactured and shot peened samples. To get a comprehensive comparison between different shot peening techniques, where three different parameters are taken into consideration: the mean arithmetic roughness (S_a), root mean square roughness (S_q), and maximum peak-to-valley height (S_{pv}) for better comparability and complete understanding of the surface.

$$S_a = \frac{1}{A} \times \iint_0^A |f(x,y)| dxdy \tag{1}$$

$$S_q = \sqrt{\frac{1}{A} \times \iint_0^A f(x,y)^2 dxdy} \tag{2}$$

$$S_{pv} = (|Max\ peak\ height| + |Max\ valley\ depth|) \tag{3}$$

where $f(x, y)$ is the function, which denotes the areal profile of the surface, and A is the area of analysis by the profilometer. The term S_a is used as the baseline for comparison and is a widely accepted and standardized parameter for roughness based on ISO 4287 [31].

3. Results and Discussion

There are four different surfaces per section with specific orientations of the truncheon sample, as shown in *Figure 3*. There are two equivalent surfaces for each orientation for both up-skins and down-skins. Therefore, there are ten surfaces for up-skins with orientations from 0 to 90° and nine surfaces for down-skins with orientations ranging from 10 to 90°.

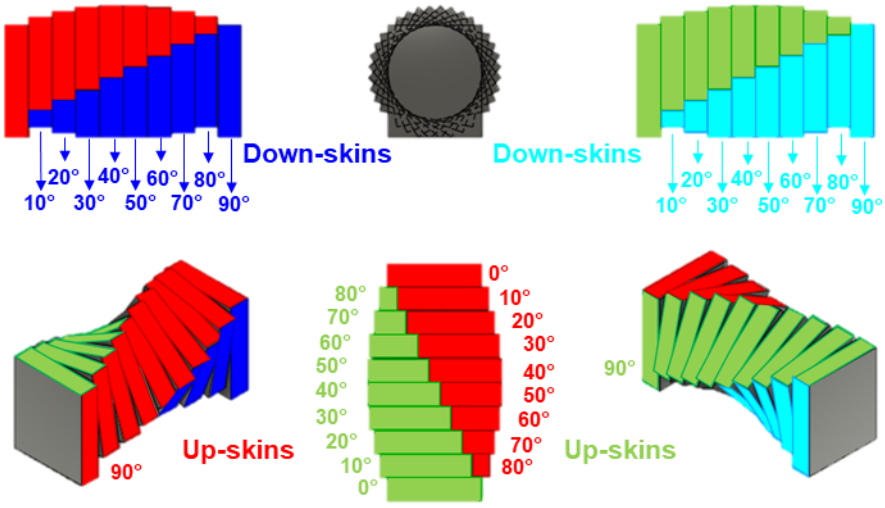

Figure 3: Representation of up-skins and down-skins in the sample design layout.

The surface roughness of the as-printed truncheon sample exhibits consistent roughness across all orientations, ranging from 0° to 90°, with values between 8-10 µm as shown in *Figure 4(a)*. A detailed investigation focused on two distinct peening techniques, specifically gravity assisted shot peening and pneumatic shot peening, emphasizing optimizing the respective peening parameters. GASP proved highly effective for the up-skin surfaces by achieving a reduction in roughness up to 50% across all orientations, demonstrating high uniformity. On the other hand, PSP at low intensity had a negligible effect on surface roughness. When increasing the intensity, the final roughness achieved was comparable to that of GASP. In contrast, the peening process required twice the duration for down-skin surfaces compared to up-skin surfaces to achieve a similar roughness as shown in *Figure 4(b)*. Surfaces with lower inclinations (10° to 40°) exhibited higher roughness than those with higher inclinations (50° to 90°). This indicates the necessity for an extended peening duration for low-inclination down-skin surfaces to attain uniform roughness across all inclinations.

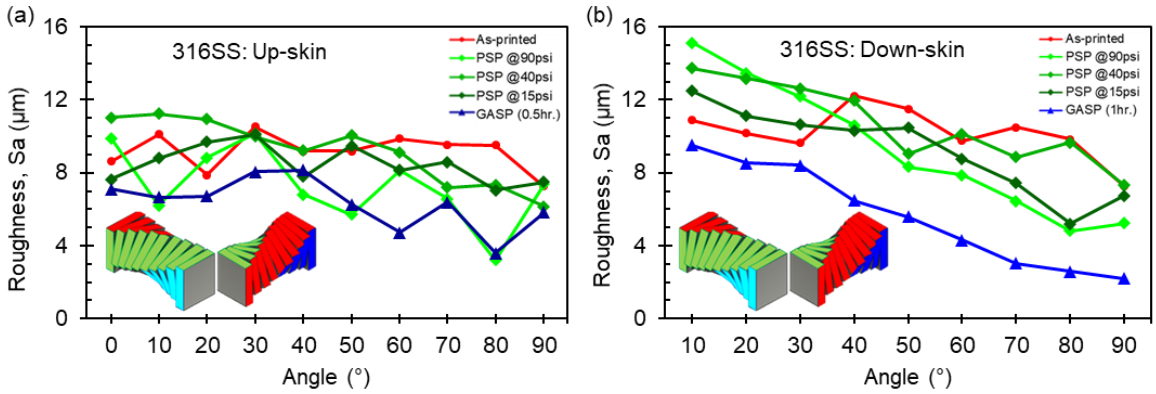

Figure 4: Areal surface roughness measurements on 316SS truncheon samples at orientations ranging from 0 to 90°: (a) up-skins and (b) down-skins.

An interesting observation regarding pneumatic shot peening was that, unlike up-skin surfaces, down-skin surfaces showed increased roughness with increasing intensity. This suggests that high-intensity PSP can lead to over-peening and cause undesirable surface damage. Although PSP was less effective in reducing roughness for low-inclination down-skin surfaces, it performed efficiently for high-inclination down-skin surfaces, achieving up to 50% effectiveness compared to GASP. For up-skin surfaces, PSP reached the same final roughness as achieved with GASP when performed at higher intensities. These findings demonstrate the importance of understanding surface topography through optical profilometry, as illustrated in *Figure 5*, to comprehend the improvements in surface features pre- and post-peening. The as-printed sample exhibits a distinct raster pattern characteristic of AM surfaces, effectively minimized by GASP, reducing roughness by up to 30% for up-skin surfaces and 45 % for down-skin surfaces. This effect was consistently observed across all orientations from 0° to 90°. For PSP, the average surface roughness across all orientations initially decreased at 15 psi, increased at 40 psi, and decreased again at 90 psi. This variation was attributed to the differential impact of peening at different orientations, where lower-inclination surfaces responded differently than higher-inclination surfaces. The topography analysis of PSP at 15 and 40 psi reveals that roughness reduction was more efficient on low-angled surfaces while high-inclination surfaces retained the as-printed surface features. However, at 90 psi, the effect of PSP was more uniform across all orientations, similar to the results achieved with GASP. This uniformity at 90 psi is likely due to the matching peening intensity of 7A, which aligns with the intensity used in GASP.

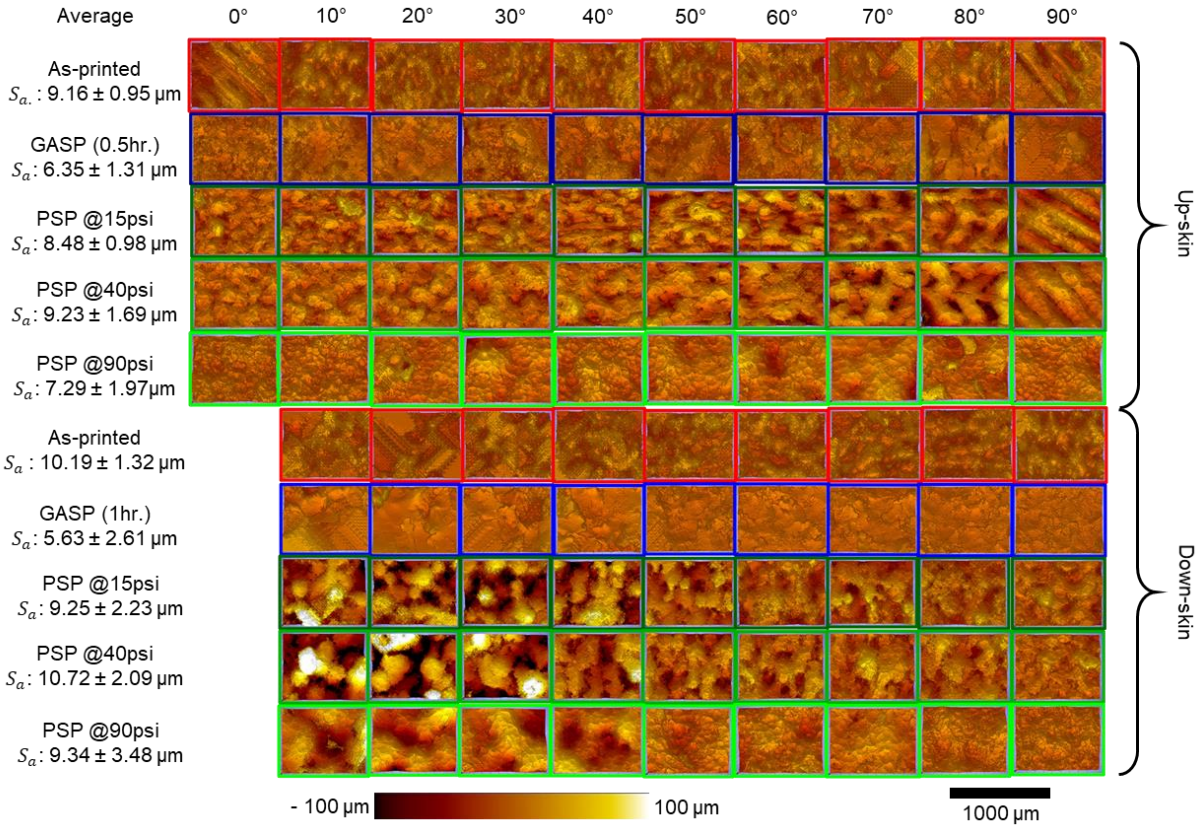

Figure 5: Surface topography of as-printed, gravity assisted shot peened, and pneumatic shot peened surfaces at different peening conditions.

In the case of down-skins, the number of peaks and valleys in the topology decreased with increasing inclination. These observations on up-skin surfaces contrary to the down-skin surfaces, exhibit a markedly different trend primarily due to the significant influence of gravity and the impact of the recoating blade during the additive manufacturing process. These factors contribute to dross formation resulting in inferior surface quality. Consequently, there is increased variability in surface roughness and an elevated risk of damage from peening processes. In the case of GASP, the technique generally produces more uniform plastic deformation, effectively reducing peaks and valleys on down-skin surfaces similar to the observations made for up-skin surfaces. This uniformity in deformation contributes to a more consistent surface finish, mitigating the adverse effects caused by the initial poor surface quality of down-skin areas.

4. Conclusions

These findings highlight the differential impact of peening techniques and intensities on surface roughness, emphasizing the need for tailored approaches based on surface orientation and inclination. Based on the experimental results, the following conclusions can be drawn:

- Gravity assisted shot peening (GASP) achieved uniform surface roughness reduction in both up-skin and down-skin surfaces, with efficiency improvements of up to 30% and 45%, respectively.
- Pneumatic shot peening (PSP) exhibited varying effectiveness based on the surface orientation.
- For up-skin surfaces, increasing the peening intensity in PSP resulted in improved roughness reduction. At the maximum intensity of 90 psi, the surface roughness achieved was comparable to that of GASP.
- For down-skin surfaces, the effect of PSP intensity showed divergent trends based on the inclination angle:
    - Low-inclination down-skins (10° to 40°): Roughness increased with higher PSP intensity.
    - High-inclination down-skins (50° to 90°): Roughness decreased with increasing PSP intensity, and at the highest intensity, the roughness values matched those achieved with GASP.

Acknowledgments

The authors thank Matsuura USA for helping to manufacture the samples of interest, and Progressive Surfaces and Sinto America for their helping with the gravity assisted shot peening (GASP) and pneumatic shot peening (PSP) processes, respectively. The Center for Surface Engineering and Enhancement in the School of Materials Engineering at Purdue University financially supported this work.

References

[1] I. Gibson, D. Rosen, B. Stucker, and M. Khorasani, “Additive Manufacturing Technologies”. vol. 17, pp. 160-186, 2021. Cham, Switzerland: Springer.

[2] X. Lin and W. Huang, “High performance metal additive manufacturing technology applied in aviation field,” *Materials China*, vol. 34, no. 9, pp. 684–688, 2015, doi: 10.7502/J.ISSN.1674-3962.2015.09.06.

[3] M. Wiese, S. Thiede, and C. Herrmann, “Rapid manufacturing of automotive polymer series parts: A systematic review of processes, materials and challenges,” *Addit Manuf*, vol. 36, p. 101582, 2020, doi: 10.1016/J.ADDMA.2020.101582.

[4] C. Culmone, G. Smit, and P. Breedveld, “Additive manufacturing of medical instruments: A state-of-the-art review,” *Addit Manuf*, vol. 27, p. 461–473, 2019, doi: 10.1016/j.addma.2019.03.015.

[5] International Organization for Standardization. (2021). Additive manufacturing — General principles — Fundamentals and vocabulary (ISO Standard No. 52900:2021(en)) Available: https://www.iso.org/obp/ui/#iso:std:iso-astm:52900:ed-2:v1:en

[6] A. Dolenc, I. Mäkelä, “Slicing procedures for layered manufacturing techniques," *Computer-Aided Design*, vol. 26, no. 2, p. 119-126, 1994.

[7] P.C. Priarone, V. Lunetto, E. Atzeni, and A. Salmi, “Laser powder bed fusion (L-PBF) additive manufacturing: On the correlation between design choices and process sustainability,” *Procedia CIRP*, vol. 78, pp. 85–90, Jan. 2018, doi: 10.1016/J.PROCIR.2018.09.058.

[8] I. Yadroitsev, “Selective laser melting: Direct manufacturing of 3D-objects by selective laser melting of metal powders,” *Appl Catal B*, vol. 75, no. 3–4, pp. 1–266, 2009.

[9] H.Y. Chia, J. Wu, X. Wang, W. Yan, “Process parameter optimization of metal additive manufacturing: a review and outlook,” *J. Materials Informatics*, vol. 2, no. 3, p. 16, 2022, doi: 10.20517/JMI.2022.18.

[10] Y. Qin, S. Lou, P. Shi, Q. Qi, W. Zeng, P.J. Scott, X. Jiang, “Optimisation of process parameters for improving surface quality in laser powder bed fusion,” *Intl. J. Adv. Manufacturing Tech.*, vol. 130, no. 5–6, pp. 2833–2845, 2024, doi: 10.1007/S00170-023-12826-8/TABLES/5.

[11] Z. Zhang, Y. Wang, P. Ge, T. Wu, “A Review on Modelling and Simulation of Laser Additive Manufacturing: Heat Transfer, Microstructure Evolutions and Mechanical Properties,” *Coatings*, vol. 12, no. 9, p. 1277, 2022, doi: 10.3390/COATINGS12091277.

[12] G. Rasiya, A. Shukla, K. Saran, “Additive Manufacturing - A Review,” Materials Today: Proceedings, vol. 47, p. 6896-6901, 2021, doi: 10.1016/j.matpr.2021.05.181.

[13] W. Wang, H. Garmestani, and S. Y. Liang, “Prediction of Upper Surface Roughness in Laser Powder Bed Fusion,” *Metals*, vol. 12, no. 1, p. 11, 2021, doi: 10.3390/MET12010011.

[14] M. Li, D. Andersson, R. Dehoff, A. Jokisaari, I. van Rooyen, D. Cairns-Gallimore, “Advanced Materials and Manufacturing Technologies (AMMT) 2022 Roadmap”, No. ANL-23/12. Argonne National Lab (ANL), Argonne, IL (United States). Available: www.anl.gov.

[15] M.J. Mirzaali, N. Shahriari, J. Zhou, A.A. Zadpoor, "Quality of AM implants in biomedical application," *Quality Analysis of Additively Manufactured Metals: Simulation Approaches, Processes, and Microstructure Properties*, pp. 689–743, 2023, doi: 10.1016/B978-0-323-88664-2.00015-4.

[16] M. Laleh, A.E. Hughes, S. Yang, J. Wang, J. Li, A.M. Glenn, W. Xu, M.Y. Tan, "A critical insight into lack-of-fusion pore structures in additively manufactured stainless steel," *Addit Manuf*, vol. 38, p. 101762, 2021, doi: 10.1016/J.ADDMA.2020.101762.

[17] M. Hemachandra, S. Thapliyal, K. Adepu, "A review on microstructural and tribological performance of additively manufactured parts," *J. Mater Sci*, vol. 57, no. 36, pp. 17139–17161, 2022, doi: 10.1007/S10853-022-07736-1/METRICS.

[18] P. O'Hara, "Peen-forming–a developing technique," *Shot Peening*, pp. 215–226, 2002, Available: https://books.google.com/books/ about/Shot_Peening.html?id=x8IkfEC4VUEC

[19] H. Kumar, S. Singh, P. Kumar, "Modified shot peening processes – A review," *Intl. J. Eng. Sci. & Emerging Technologies*, vol. 5, no. 1, pp. 12–19, 2013.

[20] A. Niku-Lari, "Overview on the shot peening process," *Advances in surface treatments*, pp. 155–170, 1987, doi: 10.1016/B978-0-08-034923-7.50023-1.

[21] Metal Improvement Company, "Shot Peening Applications" 9th edition, Curtis-Wright Corporation, p. 1-60, 2005, Paramus, NJ, USA. www.metalimprovement.com

[22] T. Gundgire, T. Jokiaho, S. Santa-aho, T. Rautio, A. Järvenpää, M. Vippola, "Comparative study of additively manufactured and reference 316 L stainless steel samples - Effect of severe shot peening on microstructure and residual stresses," *Mater Charact*, vol. 191, p. 112162, 2022, doi: 10.1016/J.MATCHAR.2022.112162.

[23] R. Żebrowski, M. Walczak, "The effect of shot peening on the corrosion behaviour of Ti-6Al-4V alloy made by DMLS," *Advances in Materials Science*, vol. 18, no. 3, pp. 43–54, 2018, doi: 10.1515/ADMS-2017-0040.

[24] M. Sugavaneswaran, A. Vinoth Jebaraj, B. Kumar, K. Lokesh, A.J. Rajan, "Enhancement of surface characteristics of direct metal laser sintered stainless steel 316L by shot peening," *Surfaces and Interfaces*, vol. 12, p. 31-40, 2018. doi: 10.1016/j.surfin.2018.04.010.

[25] E. Maleki, O. Unal, · Kazem, R. Kashyzadeh, "Influences of Shot Peening Parameters on Mechanical Properties and Fatigue Behavior of 316 L Steel: Experimental, Taguchi Method and Response Surface Methodology," *Metals and Materials International*, vol. 27, pp. 4418–4440, 2021, doi: 10.1007/s12540-021-01013-7.

[26] A. Behjat, M. Shamanian, A. Taherizadeh, M. Noori, E. Lannunziata, L. Iuliano, A. Saboori, "Enhanced surface properties and bioactivity of additively manufactured 316L stainless steel using different post-treatments." *Materials Today: Proceedings*, vol. 70, p. 188-194, 2022. doi: 10.1016/j.matpr.2022.09.019.

[27] T. Klotz, D. Delbergue, P. Bocher, M. Lévesque, M. Brochu, "Surface characteristics and fatigue behavior of shot peened Inconel 718," *Intl. J. Fatigue*, vol. 110, p.10-21, 2018. doi: 10.1016/j.ijfatigue.2018.01.005.

[28] S. Bagherifard, S. Slawik, I. Fernández-Pariente, C. Pauly, F. Mücklich, M. Guagliano, "Nanoscale surface modification of AISI 316L stainless steel by severe shot peening," *Materials & Design*, vol. 102, p. 68-77, 2016, doi: 10.1016/j.matdes.2016.03.162.

[29] Q. Zhong, K. Wei, T. Ouyang, X. Li, X. Zeng, “Effect of rotation angle on surface morphology, microstructure, and mechanical properties of Inconel 718 alloy fabricated by high power laser powder bed fusion,” *J Mater Sci Technol*, vol. 154, pp. 30–42, 2023, doi: 10.1016/J.JMST.2023.01.021.

[30] A. Liang, K.S. Pey, T. Polcar, A.R. Hamilton, “Effects of rescanning parameters on densification and microstructural refinement of 316L stainless steel fabricated by laser powder bed fusion,” *J Mater Process Technol*, vol. 302, p. 117493, 2022, doi: 10.1016/J.JMATPROTEC.2022.117493.

[31] International Organization for Standardization. (2021). Geometrical product specifications (GPS) - Surface texture: Profile (ISO Standard No. 21920-2:2021) Available: https://www.iso.org/standard/72226.html.